# Confronting Lemaitre-Tolman-Bondi models with Observational Cosmology

**Juan Garcia-Bellido**[1,2]**, Troels Haugbølle**[1,3]

[1] Instituto de Física Teórica UAM-CSIC, Universidad Autónoma de Madrid, Cantoblanco, 28049 Madrid, Spain,
[2] Kavli Institute for Theoretical Physics, University of California Santa Barbara, CA 93106-4030,
[3] Department of Physics and Astronomy, University of Aarhus, DK-8000 Aarhus C, Denmark

E-mail: `juan.garciabellido@uam.es, haugboel@phys.au.dk`

**Abstract.** The possibility that we live in a special place in the universe, close to the centre of a large void, seems an appealing alternative to the prevailing interpretation of the acceleration of the universe in terms of a $\Lambda$CDM model with a dominant dark energy component. In this paper we confront the asymptotically flat Lemaitre-Tolman-Bondi (LTB) models with a series of observations, from Type Ia Supernovae to Cosmic Microwave Background and Baryon Acoustic Oscillations data. We propose two concrete LTB models describing a local void in which the only arbitrary functions are the radial dependence of the matter density $\Omega_M$ and the Hubble expansion rate $H$. We find that all observations can be accommodated within 1 sigma, for our models with 4 or 5 independent parameters. The best fit models have a $\chi^2$ very close to that of the $\Lambda$CDM model. A general Fortran program for comparing LTB models with cosmological observations, that has been used to make the parameter scan in this paper, is made public, and can be downloaded at `http://www.phys.au.dk/~haugboel/software.shtml` together with `IDL` routines for creating the Likelihood plots. We perform a simple Bayesian analysis and show that one cannot exclude the hypothesis that we live within a large local void of an otherwise Einstein-de Sitter model.

## 1. Introduction

Cosmology has been traditionally prone to speculation, a science which has had more of wishful thinking than actual deduction. Even today, with the extraordinary revolution in observational cosmology, there are many assumptions we have to take for granted, in order to *interpret* the present observations. In particular, the present abundance of less that 5% of critical density in matter we know and measure in the laboratory, i.e. the baryons we are made of, compared to the 23% of unknown "dark matter" and the 72% of even more unknown "dark energy", seems a rather peculiar and perhaps suspicious composition for the universe, given their disparate evolution rates. Are we sure we have now the correct picture of the universe?

We live in a very isolated part of the universe and have not reached that much beyond our solar system. All we can say about the universe has been inferred from observations done under very general assumptions; but some of them, no matter how fundamental they may seem, may be wrong. It is worth pointing out how Einstein failed to make one of the most fundamental predictions of his new theory of general relativity, and had to introduce an "absolute" in the theory − the cosmological constant − much to his regret, because he had the prejudice, supported by incomplete observational data, that we lived in a static universe without a beginning or an end. Soon after the discovery of the "recession" of galaxies by Hubble did he renounce to his prejudice on the validity of the Perfect Cosmological Principle, which assumed maximally symmetric space-times. For 70 years cosmologists have worked under the assumption of the less strict Cosmological Principle, which imposes maximal symmetry (homogeneity and isotropy) only for the spatial sections. But are these symmetries consistent with observations? It is evident to anyone that looks at the sky in a clear night far away from city lights that the universe is *not* homogeneous and isotropic.

It has usually been argued that these fundamental symmetries should only be "expected to be valid on very large scales", but how *large* are large scales? In fact, the distribution of matter in our local vicinity, i.e. within several Mpc, is very far from homogeneous; density contrasts reach enormous values not only at the centres of galaxies but also on larger scales like clusters and superclusters, stretching over hundreds of Mpc. So, how far do we have to go before we reach homogeneity? Certainly present galaxy catalogues are not really there yet, and it has been speculated that perhaps with the next generation of deep catalogues like DES [1] we will finally reach the homogeneity limit. But, if we do *not* live in a homogeneous universe, how do we interpret the observations we have of objects whose light has travelled a significant fraction of the age of the universe in order to reach us? Our present assumption is that, in practice, the intervening inhomogeneity averages out and everything works as if we lived in a homogeneous universe. For several decades this assumption has been a valid one, and has provided confidence into the construction of the so-called Standard Model of Cosmology.

It is only now that we begin to have sufficiently good cosmological data, and certainly will have even better data in the near future, that we can be critical

and pose the appropriate questions. The issue of homogeneity of the universe has been often dismissed because of the apparent extraordinary isotropy of the cosmic microwave background. However, any mathematician can readily show that isotropy and homogeneity are very different sets of symmetries and one does not imply the other. Nevertheless, if we impose the further assumption, usually stated as the Copernican Principle, that any point in space should be equivalent to any other, i.e. that we don't live in any special place in the universe, then a mathematical theorem states that if *all* equal observers see the universe isotropic around them, then the universe must be not only isotropic but also homogeneous. What remains to be proven is that all observers are in fact equivalent in the patch of the universe we call the observable universe. Some will be near a large concentration of mass and others will be in large voids. Certainly what these two types of observers see will differ from what an idealised observer living in a perfectly homogeneous universe would see. Unfortunately, we have never spoken to anyone at the other side of the universe.

The advantage of the present state of Cosmology is that we can begin to pose those questions and hope to get concrete answers, while just ten years ago it would have been futile. Moreover, like with the first inclusion of the cosmological constant in the theory, almost 100 years ago, the physics community is very much puzzled about the nature of this so-called vacuum energy. Its properties defy our basic understanding of quantum physics and, moreover, it reminds us suspiciously of the Maxwellian ether, which led the way (via its disappearance) to a new understanding of physical reality. To put the question straight, are we sure we live in an accelerated universe which is driven by some unknown vacuum energy? Could it be that we have *misinterpreted* our superb cosmological data and what those photons coming from afar are telling us is something completely different?

The last few years we have seen a tremendous burst of activity, both at the theoretical and observational level, in order to disentangle the subtle intricacies of the actual data sets from their interpretation. As with any hard science (and Cosmology is indeed finally becoming one), such enterprises can be approached only via further observational crosschecks. It is no longer true that "astrophysicists are often in error, but never in doubt", as Lev Landau once said to annoy his colleague Yakov Zel'dovich [2]. We can now propose new ways to measure more observables in a wider theoretical construction. Perhaps it is time to explore the troubled waters of non-maximally symmetric spatial sections of the universe. In particular, since we indeed observe a high degree of isotropy in the cosmic microwave background, we can start by exploring the simplified version of a spherically symmetric inhomogeneous model, which comes under the name of the Lemaître-Tolman-Bondi (LTB) model [3, 4, 5].

While ordinary Friedmann-Robertson-Walker (FRW) space-times are characterised by two functions, the Hubble rate $H(t)$ and the density parameter $\Omega(t)$, which depend on cosmic time but are independent of the radial coordinate, the LTB models have also two arbitrary functions, $H(r,t)$ and $\Omega(r,t)$, which depend on both time and the radial coordinate. The Einstein equations for the LTB model are sufficiently simple that they

can be integrated exactly in terms of two arbitrary boundary conditions. Thus, the LTB models have lower symmetries, and thus more freedom, but nevertheless make specific predictions about the behaviour of light along geodesics of the new metric. Therefore, one can evaluate the corresponding observables, like cosmological distances (or ratios of distances), from the available sets of data. Surprisingly, as we will show in the next sections, present cosmological data does not yet seem able to exclude with confidence a universe which is not exactly homogeneous. This should not come as a surprise, we *do* live in an (locally) inhomogeneous universe, some say that within a large underdense void [6, 7, 8, 9, 10, 11] similar to that which induces a cold spot in the CMB [12, 13, 14] so why should we assume global homogeneity? In fact, the possibility that we happen to live in the centre of the world was advocated long ago in Ref. [15], based on the stochastic inflation formalism [16, 17]. What is surprising is that within this framework one can account for (almost) all observational evidence without having to introduce an unknown in the theory, an absolute, whose properties are highly mysterious, not to mention the alternative highly artificial and ad hoc modifications of gravity on the very large scales.

In this paper we propose an inhomogeneous model of the universe, with a local void size of a few Gpc and asymptotically Einstein-de Sitter, and then use the present sets of data (CMB, LSS, BAO, SNIa, HST, Ages, etc.) to constrain its parameters. In Section 2 we describe the general LTB metric, the Einstein equations and the definitions of cosmic distances. We also give a novel series expansion that allows one to integrate to arbitrary precision the Einstein equations for arbitrary functions $H_0(r)$ and $\Omega_M(r)$. We then describe a specific model with a concrete form of these two functions that are plausible but simple matches to observations, and show the different (longitudinal and transverse) rates of expansion and the apparent acceleration. We also show that the comoving size of the sound horizon depends on the distance to the centre of the void in the LTB model, and relate it to the expansion rates at different redshifts. This is a prerequisite for making a realistic comparison with Baryon Acoustic Oscillation data. In Sect. 3 we present the data sets we use to constrain the model, with the subtleties needed to correctly interpret these in terms of the model. In Sect. 4 we give the main results and present a Bayesian analysis to ascertain the goodness of fit of the model by comparing it with a standard $\Lambda$CDM model with variable (but constant) equation of state parameter $w$. In Sect. 5 we give the conclusions.

## 2. The LTB model

The most general (cosmological) metric satisfying spherically symmetric spatial sections can be written as

$$ds^2 = -dt^2 + X^2(r,t)\, dr^2 + A^2(r,t)\, d\Omega^2 \,, \tag{1}$$

where $d\Omega^2 = d\theta^2 + \sin^2\theta d\phi^2$. Assuming a spherically symmetric matter source,

$$T^\mu_\nu = -\rho_M(r,t)\, \delta^\mu_0\, \delta^0_\nu,$$

the $(0, r)$ component of the Einstein equations, $G_r^0 = 0$, implies $X(r, t) = A'(r, t)/\sqrt{1 - k(r)}$, with an arbitrary function $k(r)$ playing the role of the spatial curvature parameter. Note that we recover the FRW metric imposing the extra homogeneity conditions,

$$A(r, t) = a(t)\, r\,, \qquad\qquad k(r) = k\, r^2\,.$$

The other components of Einstein equations read[18, 19]

$$\frac{\dot{A}^2 + k}{A^2} + 2\frac{\dot{A}\dot{A}'}{AA'} + \frac{k'(r)}{AA'} = 8\pi\, G\, \rho_M\,, \tag{2}$$

$$\dot{A}^2 + 2A\ddot{A} + k(r) = 0\,. \tag{3}$$

Integrating the last equation, we get

$$\frac{\dot{A}^2}{A^2} = \frac{F(r)}{A^3} - \frac{k(r)}{A^2}\,, \tag{4}$$

with another arbitrary function $F(r)$, playing the role of effective matter content, which substituted into the first equation gives

$$\frac{F'(r)}{A'A^2(r, t)} = 8\pi\, G\, \rho_M(r, t)\,. \tag{5}$$

Combining these two equations we arrive at

$$\frac{2}{3}\frac{\ddot{A}}{A} + \frac{1}{3}\frac{\ddot{A}'}{A'} = -\frac{4\pi\, G}{3}\, \rho_M\,, \tag{6}$$

which determines the "effective" acceleration in these inhomogeneous cosmologies. Note that the notion of acceleration becomes ambiguous since backward proper time has both a time and a spatial component.

The boundary condition functions $F(r)$ and $k(r)$ are specified by the nature of the inhomogeneities through the local Hubble rate, the local matter density and the local spatial curvature,

$$H(r, t) = \frac{\dot{A}(r, t)}{A(r, t)}\,, \tag{7}$$

$$F(r) = H_0^2(r)\, \Omega_M(r)\, A_0^3(r)\,, \tag{8}$$

$$k(r) = H_0^2(r)\Big(\Omega_M(r) - 1\Big)\, A_0^2(r)\,, \tag{9}$$

where functions with subscripts 0 correspond to present values, $A_0(r) = A(r, t_0)$ and $H_0(r) = H(r, t_0)$. With these definitions, the $r$-dependent Hubble rate is written as[18, 19]

$$H^2(r, t) = H_0^2(r)\left[\Omega_M(r)\left(\frac{A_0(r)}{A(r, t)}\right)^3 + (1 - \Omega_M(r))\left(\frac{A_0(r)}{A(r, t)}\right)^2\right]\,. \tag{10}$$

Inhomogeneities come in two different classes: in the matter distribution or in the expansion rate, which are mutually independent. Moreover, the extra gauge freedom of the synchronous comoving gauge allows us to choose

$$A(r, t_0) = A_0(r) = r\,. \tag{11}$$

Then we can integrate the Hamiltonian constraint equation (10) to provide comoving time as a function of the radial coordinate,

$$
H_0(r)t(r) = \int^{A(r,t)/A_0(r)} \frac{dx}{\sqrt{\Omega_M(r)/x + 1 - \Omega_M(r)}}
$$

$$
= \frac{A(r,t)}{A_0(r)\sqrt{\Omega_K(r)}}\sqrt{1 + \frac{\Omega_M(r)A_0(r)}{\Omega_K(r)A(r,t)}} - \frac{\Omega_M(r)}{\sqrt{\Omega_K^3(r)}}\sinh^{-1}\sqrt{\frac{\Omega_K(r)A(r,t)}{\Omega_M(r)A_0(r)}}, \quad (12)
$$

where $\Omega_K(r) = 1 - \Omega_M(r)$. In particular, setting $A(r,t) = A_0(r)$ we find the current age of the universe

$$
H_0(r)t_{\rm BB}(r) = \frac{1}{\sqrt{\Omega_K(r)}}\sqrt{1 + \frac{\Omega_M(r)}{\Omega_K(r)}} - \frac{\Omega_M(r)}{\sqrt{\Omega_K^3(r)}}\sinh^{-1}\sqrt{\frac{\Omega_K(r)}{\Omega_M(r)}}. \quad (13)
$$

For an observer located at the centre $r = 0$, by symmetry, incoming light travels along radial null geodesics, $ds^2 = d\Omega^2 = 0$, and time decreases when going away, $dt/dr < 0$, and we have

$$
\frac{dt}{dr} = -\frac{A'(r,t)}{\sqrt{1 - k(r)}} \quad (14)
$$

which, together with the redshift equation,

$$
\frac{d\log(1+z)}{dr} = \frac{\dot{A}'(r,t)}{\sqrt{1 - k(r)}} \quad (15)
$$

can be written as a parametric set of differential equations, with $N = \log(1 + z)$ being the effective number of e-folds before the present time,

$$
\frac{dt}{dN} = -\frac{A'(r,t)}{\dot{A}'(r,t)}, \quad (16)
$$

$$
\frac{dr}{dN} = \frac{\sqrt{1 - k(r)}}{\dot{A}'(r,t)}, \quad (17)
$$

from which the functions $t(z)$ and $r(z)$ can be obtained. From there one can immediately obtain both the luminosity distance, the comoving distance and the angular diameter distance as a function of redshift,

$$
d_L(z) = (1+z)^2 A[r(z), t(z)], \quad (18)
$$

$$
d_C(z) = (1+z) A[r(z), t(z)], \quad (19)
$$

$$
d_A(z) = A[r(z), t(z)], \quad (20)
$$

## 2.1. Series solution

In order to integrate out the redshift dependence it will be useful to make a series expansion of the cosmic time variable $t(r)$ as a function of the space-dependent scale factor $A(r,t)$. For this purpose we will define new variables

$$
y = \frac{\Omega_K(r)}{\Omega_M(r)} H_0(r)\sqrt{\Omega_K(r)}\, t(r) = \frac{2}{3}(\delta\, a)^{3/2}, \quad (21)
$$

$$
x = \frac{\Omega_K(r)}{\Omega_M(r)} \frac{A(r,t)}{A_0(r)} = \delta\, \frac{A}{A_0}, \quad (22)
$$

where $\delta = \rho_c/\rho_M - 1$ is the density contrast ratio and $a(t)$ is the Einstein-de Sitter (FRW) scale factor,

$$\delta(r) = \frac{\Omega_K(r)}{\Omega_M(r)}, \tag{23}$$

$$a(t) = \left(\frac{3}{2} H_0(r) \sqrt{\Omega_M(r)}\, t\right)^{2/3}. \tag{24}$$

With these definitions, the time integral (12) can be written as $y = \sqrt{x(1+x)} - \ln[\sqrt{x} + \sqrt{1+x}]$, which can be expanded in series and inverted. With the definitions

$$g(z) = z + \frac{1}{5}z^2 - \frac{3}{175}z^3 + \frac{23}{7875}z^4 - \frac{1894}{3031875}z^5 + \mathcal{O}(z^6), \tag{25}$$

$$f(r) = \frac{H_0'(r)}{H_0(r)} - \frac{\Omega_M'(r)}{\Omega_M(r)}\left(\frac{1+\Omega_M(r)/2}{1-\Omega_M(r)}\right), \tag{26}$$

$$h(r) = \frac{1}{r} + \frac{\Omega_M'(r)}{\Omega_M(r)(1-\Omega_M(r))}, \tag{27}$$

we can write the solution as a power series, whose coefficients can be calculated with arbitrary precision,

$$A(r,t) = \frac{r}{\delta}\, g(a\,\delta), \tag{28}$$

$$\dot{A}(r,t) = \frac{2}{3t}\frac{r}{\delta}\, a\,\delta\, g'(a\,\delta), \tag{29}$$

$$A'(r,t) = \frac{r}{\delta}\left[g(a\,\delta)h(r) + \frac{2}{3}\, a\,\delta\, g'(a\,\delta)\, f(r)\right], \tag{30}$$

$$\dot{A}'(r,t) = \frac{2}{3t}\frac{r}{\delta}\left[a\,\delta\, g'(a\,\delta)h(r) + \frac{2}{3}\, a\,\delta\, g'(a\,\delta)\, f(r) + \frac{2}{3}(a\,\delta)^2 g''(a\,\delta)\, f(r)\right], \tag{31}$$

$$\ddot{A}(r,t) = -\frac{F(r)}{2A^2(r,t)}, \tag{32}$$

$$\ddot{A}'(r,t) = \frac{F(r)A'(r,t)}{A^3(r,t)} - \frac{F'(r)}{2A^2(r,t)}. \tag{33}$$

These functions allow us to construct any other observable. For instance, the transverse and longitudinal rates of expansion can be written as

$$H_T(r,t) \equiv \frac{\dot{A}(r,t)}{A(r,t)}, \tag{34}$$

$$H_L(r,t) \equiv \frac{\dot{A}'(r,t)}{A'(r,t)}. \tag{35}$$

Note that in general these two functions will be different, and they enter into other observables. We can also construct quantities like the "effective" acceleration parameter

$$q(z) = -1 + \frac{d\,\ln H(z)}{d\,\ln(1+z)}, \tag{36}$$

where $H(z)$ is in fact $H_L(r(z), t(z))$.

One could also define an effective equation of state parameter

$$w(z) \equiv \frac{p(z)}{\rho(z)} = -1 + \frac{1}{3} \frac{d \ln \left[ H^2(z)/H_0^2(r) - \Omega_M(r)(1+z)^3 \right]}{d \ln(1+z)}, \qquad (37)$$

where $H(z)$ is here $H_T(r(z), t(z))$.

## 2.2. Parametric solution

At fixed $r$ the $r$-dependent Hubble rate Eq. (10) is just like the normal Friedmann equation, and the standard way to explicitly solve for $A(r,t)$ is to use an additional parameter $\eta$. With the selected gauge the solution is

$$A(r,t) = \frac{\Omega_M(r)}{2[1 - \Omega_M(r)]} [\cosh(\eta) - 1] A_0(r) \qquad (38)$$

$$H_0(r)t = \frac{\Omega_M(r)}{2[1 - \Omega_M(r)]^{3/2}} [\sinh(\eta) - \eta] \qquad (39)$$

Given $r$ and $t$ solving Eq. (39) $\eta$ can be found, and combining Eqs. (38)-(39) with the Einstein equations we can the derive any necessary quantity.

We have used both the series solution, implemented in a `Mathematica` notebook, and the parametric solution, implemented as a Fortran program, to make and double check all numerical computations in this paper. The Fortran 90 program together with a set of `IDL` routines for making likelihood plots is made publicly available and can be downloaded at `http://www.phys.au.dk/~haugboel/software.shtml`.

## 2.3. The GBH model

Here we define a new type of LTB model, which is completely specified by the matter content $\Omega_M(r)$ and the rate of expansion $H_0(r)$,

$$\Omega_M(r) = \Omega_{\mathrm{out}} + \left( \Omega_{\mathrm{in}} - \Omega_{\mathrm{out}} \right) \left( \frac{1 - \tanh[(r - r_0)/2\Delta r]}{1 + \tanh[r_0/2\Delta r]} \right), \qquad (40)$$

$$H_0(r) = H_{\mathrm{out}} + \left( H_{\mathrm{in}} - H_{\mathrm{out}} \right) \left( \frac{1 - \tanh[(r - r_0)/2\Delta r]}{1 + \tanh[r_0/2\Delta r]} \right), \qquad (41)$$

which is governed by 6 parameters,

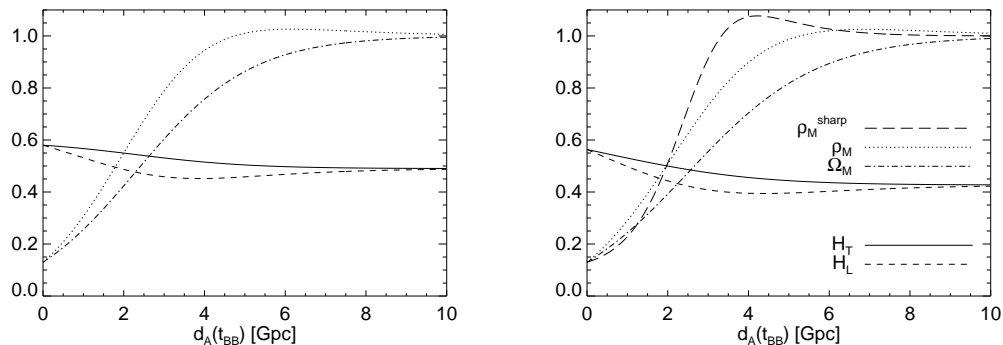| | | |
|---|---|---|
| $\Omega_{\mathrm{out}}$ | determined by asymptotic flatness | (42) |
| $\Omega_{\mathrm{in}}$ | determined by LSS observations | (43) |
| $H_{\mathrm{out}}$ | determined by CMB observations | (44) |
| $H_{\mathrm{in}}$ | determined by HST observations | (45) |
| $r_0$ | characterises the size of the void | (46) |
| $\Delta r$ | characterises the transition to uniformity | (47) |

**Figure 1.** The radial dependence of the physical matter density in units of the critical density ($\rho_m$), of our density function ($\Omega_m$), that coincides with the usual matter density at the centre and asymptotically, and of the transverse and longitudinal expansion rates ($H_T$ and $H_L$). The radial axis is the angular diameter distance ($d_A(r, t_{\rm BB})$), and everything is taken at the current time for the central observer. To the left (right) is shown the best fit GBH (constrained) model (see table 2). Also shown to the right is an example of the density profile of a model with a sharp transition ($\Delta r/r_0 = 0.3$), but still within 1-$\sigma$ of the best fit.

We fix $\Omega_{\rm out} = 1$ and let the other five parameters vary freely in our parameter scans (see table 1 for the priors). For instance, a plot of $\Omega_M(r)$, $H_T(r)$ and $H_L(r)$ for the two best fit models, as a function of the angular diameter distance today, $d_A(r, t_{\rm BB})$, can be seen in Fig. 1‡. Also shown is the density profile of a model with a sharper transition ($\Delta r/r_0 = 0.3$), but still within 1-$\sigma$ of the best fit. This illustrates that observations allow for shallower density profiles close to the origin, and that for the physical matter density $\rho_M$, we naturally get a shell-like transition.

### 2.4. The constrained GBH model

We have also considered a more constrained model, in which the Big Bang is homogeneous, that is, the spatial hypersurface at the Big Bang does not depend on the radial coordinate $r$. This can be obtained simply using Eq. (13), by a choice of $H_0(r)$,

$$H_0(r) = H_0 \left[ \frac{1}{\Omega_K(r)} - \frac{\Omega_M(r)}{\sqrt{\Omega_K^3(r)}} \sinh^{-1} \sqrt{\frac{\Omega_K(r)}{\Omega_M(r)}} \right] , \qquad (48)$$

so that $t_{\rm BB} = c\, H_0^{-1}$ is universal, for all observers, irrespective of their spatial location. Note that in this model we have less freedom than in the previous model, since now there is only one arbitrary function, $\Omega_M(r)$, and there is one free parameter less.

‡ Note that while apparently this model is similar to that of Ref. [20], it differs in the details. They fix their gauge $A(r, t) = A_0(r) = r$ at the moment of recombination, while we fix it at the current time, and they define their free functions in terms of $F(r)$ and $k(r)$, while we use $H(r)$ and $\Omega(r)$.

## 2.5. Apparent acceleration in the light cone

It is yet not clear, if what we observe as a function of redshift, in the form of luminosity distances to standard candles (e.g. Supernovae Type Ia), angular diameter distances to standard rulers (e.g. Baryon Acoustic Oscillations), the galaxy power spectrum, galaxy cluster counts, or other measures of the geometry and mass distribution of the Universe, are due to modifications of gravity, an extra energy component, a cosmological constant, or simply a wrong interpretation of the underlying cosmological model. But as a whole they represent different possible explanations for the "Dark Energy" problem. One of the main observables, that will help decide between the different scenarios in the future, is the Hubble parameter $H(z)$. *Under the assumption* that the correct background is a flat FRW cosmology we can write it [21]

$$\frac{H_{T,L}^2(z)}{H_{\text{in}}^2} = (1+z)^3 \Omega_{\text{in}} + (1-\Omega_{\text{in})} \exp\left[3\int_1^{1+z} d\log(1+z')(1+w_{\text{eff}}^{T,L}(z'))\right], \quad (49)$$

where $H_{\text{in}}$ and $\Omega_{\text{in}}$ are the expansion rate and matter density as observed at $z = 0$§. By taking the derivative we can write it as

$$w_{\text{eff}}^{T,L}(z) = -1 + \frac{1}{3}\frac{d\log\left[\frac{H_{T,L}^2(z)}{H_{\text{in}}^2} - (1+z)^3\Omega_{\text{in}}\right]}{d\log[1+z]}, \quad (50)$$

where we have assumed that $\frac{H_{T,L}^2(z)}{H_{\text{in}}^2} - (1+z)^3\Omega_{\text{in}} > 0$. The beauty of Eq. (50) is that if the observational data indeed is a manifestation of extra energy components, $w_{\text{eff}}^{T,L}(z)$ has the usual interpretation of a dark energy equation of state, while in the case of modified gravity models, or the LTB model that we are considering in this paper, it can be interpreted as an empirical observational signature. In those case $w_{\text{eff}}^{T,L}(z)$ is a function that captures the difference between the expansion rate that we measure, and the expansion rate that we ascribe to the *observed* matter density $\Omega_m$ (see also Eq. 37 for a correct definition of $w$ in the case of an LTB universe).

It is worthwhile pointing out, that even if there is not an accelerated expansion in the LTB models we are considering, because data is observed in the light cone, the total time derivative is [19]

$$\frac{D}{Dt} = \frac{\partial}{\partial t} - \frac{c\sqrt{1-k(r)}}{A'(r,t)}\frac{\partial}{\partial r} \simeq \frac{\partial}{\partial t} - c\frac{\partial}{\partial r}, \quad (51)$$

and an observer can measure an *apparent* acceleration when the light cone traverses the central inhomogeneity due to spatial gradients in either the matter density or the expansion rate. In Fig. 2 we show $w_{\text{eff}}^{T,L}(z)$ for two best fit models. Letting $H = H_T$ and $H = H_L$ are both relevant, because different observations probe different expansion rates, i.e. as will be seen below, the Baryon Acoustic Oscillation signal depends partly on $H_L$, while supernova observations are only related to $H_T$ through its dependence on $d_L = (1+z)^2 d_A = (1+z)^2 \exp(\int H_T dt)$. Interestingly, the variation and derivative of

---

§ Alternatively, in [22] Eq. (50) is written with derivatives of the scale factor $a$ instead of the redshift $z$. We advocate using $z$, as it is an observable, in contrast to $a(z)$. Notice that $H_T(0,t) = H_L(0,t)$.
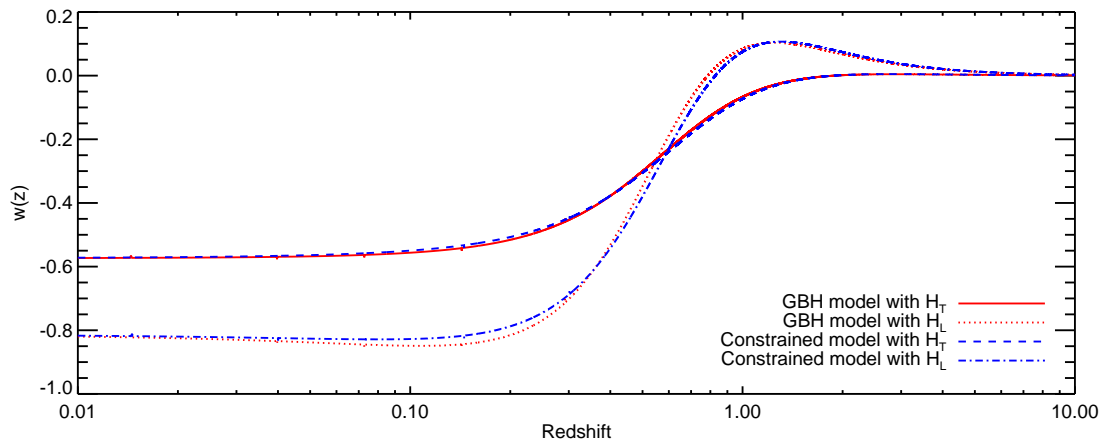
**Figure 2.** The apparent acceleration $w_{\text{eff}}^{T,L}(z)$ inferred by applying Eq. (50) and FRW cosmology as the underlying model to describe the change in the Hubble parameter (either $H_T(z)$ or $H_L(z)$) in the two best fit LTB models.

$w_{\text{eff}}^{T,L}(z)$ is quite large in the best fit LTB models, showing that a precise low redshift supernova survey, such as the SDSS Supernova Survey [23], sensitive to $H_T$, or a fine grained BAO survey such as PAU [24], sensitive to $H_L$, could rule out or reinforce the models in the near future. Conversely, if a disagreement between $w$ as observed by Supernovae and $w$ as observed through the BAOs is found, this could be a hint of inhomogeneous expansion rates.

We can directly compute $w_{\text{eff}}^{T,L}(z)$ in the limiting cases $z = 0$ and $z \gg 1$ for asymptotically flat LTB models

$$
w_{\text{eff}}^{T,L}(z) = \begin{cases} -\frac{1}{3} + \frac{2}{3}\frac{cH_0'(0)}{(1-\Omega_{\text{in}})H_{\text{in}}^2} & \text{if } z = 0, \text{ and } H = H_T \\ -\frac{1}{3} + \frac{4}{3}\frac{cH_0'(0)}{(1-\Omega_{\text{in}})H_{\text{in}}^2} & \text{if } z = 0, \text{ and } H = H_L \\ 0 & \text{if } z \gg 1 \end{cases}, \tag{52}
$$

where we have used that the LTB metric converges asymptotically to a FRW metric giving $dz = -da/a$. We see that to have $w \ll -1/3$ at low $z$ implies either a significant negative gradient in $H_0(r)$, or $\Omega_{\text{in}} \sim 1$.

## 2.6. Physical scales in the early universe

Many bounds from observational cosmology, such as the sound horizon (a "standard ruler"), the CMB, and the big bang nucleosynthesis, are derived by considering scales and processes in the early universe, and are based on the implicit assumption of an underlying FRW metric. To test LTB models against these observational data we have to connect distance scales, redshifts, and expansion rates in the early universe to those observed today.

By construction, at high redshifts the LTB metric converges to a FRW metric, and the central void disappear (see Eq. 10), and physical results derived for FRW space

times still hold in the early universe, even though we are considering an LTB space time. But starting from an approximately uniform universe at a high redshift $z_e$ in the LTB model, the expansion rate and matter density become gradually inhomogeneous, and a uniform comoving physical scale $l$ in the early universe at $z_e$, for example the sound horizon, is not uniform at some later redshift $z$. In particular the comoving size at $t = t_0 = t_{\mathrm{BB}}(0)$ depends on how much relative expansion there has been at different positions since the formation of the uniform scale

$$l(r(z)) = l(r_\infty) \frac{A(r(z), t_0)}{A(r(z), t(z_e))} \frac{A(r_\infty, t(z_e))}{A(r_\infty, t_0)} \,, \tag{53}$$

where $t_0$ is the time now for the central observer, and $r_\infty$ is the radial coordinate of an observer very far away from the void. This is a consequence of defining the comoving physical scale as the scale measured at $t_0$. If instead we fixed the comoving length scales to be measured in the early universe at $t(z_e)$, then indeed $l(r(z))$ would be independent of the observer position. The convenience of the above formula is, that the LTB models we consider are asymptotically FRW, and we can easily compute comoving scales at infinity.

Normal relations determining early universe quantities, such as the redshift at matter-radiation equality, are essentially based on the Friedmann and conservation equations to relate cosmological parameters now to the parameters then

$$H^2(z) = H_0^2 \left[\Omega_M(1+z)^3 + (1 - \Omega_M)(1+z)^2\right] \tag{54}$$

$$\rho(z)a^3 = \rho(0)a_0^3 \,, \tag{55}$$

where we have written it for a matter dominated universe. Eq. (10) is the LTB equivalent to Eq. (54), and since we are considering LTB metrics that asymptotically converge to FRW metrics the equation for light rays, or null geodesics, (15) at high redshifts have the usual solution $d(1+z) = -da/a$, and we can write an asymptotic version of Eq. (10) that is valid at high redshifts

$$H^2(z) = H_{\mathrm{eff}}^2 \left[\Omega_M^{\mathrm{eff}}(1+z)^3 + (1 - \Omega_M^{\mathrm{eff}})(1+z)^2\right] \tag{56}$$

where

$$H_{\mathrm{eff}} = H_0(z_e) \left[\frac{A_0(r(z_e))}{(1+z_e)A(r(z_e), t(z_e))}\right]^{3/2} \tag{57}$$

and the asymptotic matter density is

$$\Omega_M^{\mathrm{eff}} = \Omega_M(r(z_e)) = \Omega_{\mathrm{out}} = 1 \tag{58}$$

In summary, any quantity at high redshifts in the LTB model can be computed with the usual formulas valid for a FRW metric, but using the matter density and Hubble constant given in Eqs. (57)-(58).

## 3. Observational Data

To assess the viability of the proposed models we have tested them against a set of current observational data. We divide the data into two classes: Constraining data sets,

and prior data. The constraining data sets are actual measurements with errors, that are used to compute the likelihood of a given model, while the prior data, merely give ranges inside which the models should be.

## 3.1. The Cosmic Microwave Background

It is not a priori clear how to compute the spectrum of temperature anisotropies, without a full perturbation theory for the LTB models, but as shown in section 2.6 we can compute the comoving distance to the surface of large scattering, and the comoving size of the sound horizon at large distances. The ratio give the typical size, of the CMB temperature fluctuations on the sky, or equivalently the scale of the first peak, which is measured with exquisite precision by the WMAP satellite [25]

$$\theta_{\rm CMB} = \frac{r_s(z_{\rm rec})}{d_C(z_{\rm rec})} = 0.5952 \pm 0.0021^\circ = 0.010388 \pm 0.00037. \tag{59}$$

The sound horizon $r_s(z_{\rm rec})$ is calculated using the fitting formula provided by Eisenstein and Hu [26] with $\Omega_M = \Omega_{\rm out} = 1$, $h = H_{\rm eff}$ (see Eq. 57). The physical baryon density in the early universe and the recombination redshift are fixed to their best fit WMAP3 values $\Omega_B H_{\rm eff}^2 = 0.0223$ and $z_{\rm rec} = 1089$. The $\chi^2$ from the CMB constraint is simply

$$\chi_{\rm CMB}^2 = \frac{\left[\theta_{\rm CMB} - r_s(z_{\rm rec})/(d_C(z_{\rm rec})\right]^2}{\sigma_\theta^2} \tag{60}$$

## 3.2. Baryon Acoustic Oscillations

The BAO has been measured at different scales using a variety of techniques, and the feature has been detected in the 3D two-point correlation function [27, 28], the 3D power spectrum [29], and the angular power spectrum [30]. In particular Percival et al [29] have combined the 2DF and SDSS large scale surveys to yield a measure of the BAO centred at two different redshifts, namely $z = 0.2$, and $z = 0.35$.

In [29] the power spectrum is calculated in a reference cosmology, and then the comoving distance scale is either dilated, using a fixed factor, or deformed using a 3 node spline fit. In principle one would need a full perturbation theory for LTB geometries to recalculate the 3D power spectrum, using our best fit model, but if we take into account that the observed galaxies are divided into redshift slices, and that the LTB universe at constant redshift behaves locally like a homogeneous FRW universe (e.g. Eq. (10) is a local analogy to the normal FRW Hubble rate equation), we can then, as a first approximation, relate the $\Lambda$CDM power spectrum calculated in [29] to the LTB power spectrum through a dilation. In Fig. 3 we show the fractional difference between a simple dilation of the comoving scale, and a full modelling around the relevant redshifts $z = 0.2$ and $= 0.35$. The dilation is an excellent approximation, the difference being less than 2% over the relevant redshift range. We stress, however, that a comprehensive test of LTB models against large scale structure data has to await the development of the linear perturbation theory for LTB space times, an approach that is outside the scope of this paper [31].
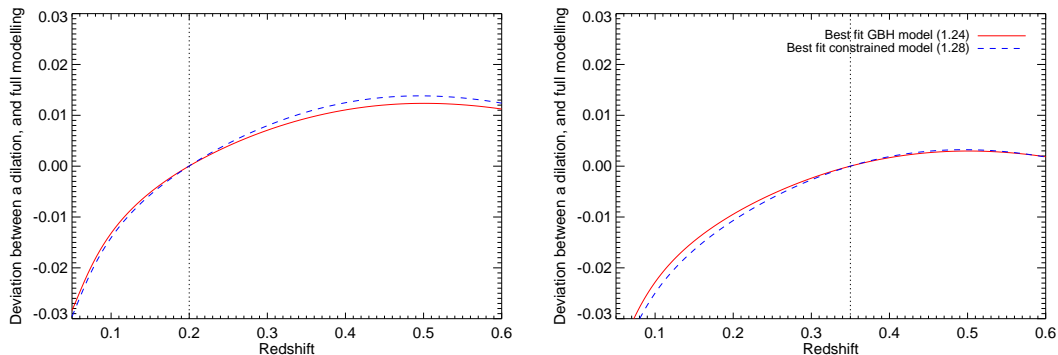
**Figure 3.** The fractional difference in the comoving distance used in the reference model in [29] compared to the best fit GBH model (red, full line) and constrained model (blue, dashed line). To the left (right) is shown the the dilation at $z = 0.2$ ($z = 0.35$), and in parenthesis in the legend is indicated the dilation.

The relevant BAO quantity to test against is the observed peak (in the case of real space) or wiggle wavelength (in the case of Fourier space), compared to the size of the sound horizon in the reference model used in [29], which can be interpreted approximately as the projected size of the BAO on the sky for structures at a given redshift. The ratio is given as

$$\theta_{BAO}(z) = \frac{r_s(z)}{D_V(z)} \,. \tag{61}$$

As discussed in Section 2.6, the *comoving* size of the sound horizon $r_s(z)$ is a function of redshift, due to the inhomogeneous nature of the expansion since the surface of last scattering $A(r(z), t(z))/A(r(z_{\rm rec}), t(z_{\rm rec}))$. Because we detect the BAO in the 3D distribution of galaxies, and not in the 2D projection on the sky, $D_V$ is not just the comoving distance, but rather a combination of longitudinal and transversal distances. In LTB space-times the longitudinal and transversal Hubble parameters, $H_L$ and $H_T$, can differ significantly, see Fig. 1, and therefore it is important to use the correct longitudinal expansion rate:

$$D_V(z) = \left[ d_A^2(z)(1 + z)^2 \frac{cz}{H_L(z)} \right]^{1/3} . \tag{62}$$

Percival et al [29] find

$$\theta_{\rm BAO}(0.2) = 0.1980 \pm 0.0058 \qquad \theta_{\rm BAO}(0.35) = 0.1094 \pm 0.0033 \tag{63}$$

with a 39% correlation, and we use these two measurements as our BAO data set giving the $\chi^2$

$$\chi^2_{\rm BAO} = \sum_{i,j} \left[ \theta_{\rm BAO}(z_i) - r_s(z_i)/D_V(z_i) \right] C_{ij}^{-1} \left[ \theta_{\rm BAO}(z_j) - r_s(z_j)/D_V(z_j) \right] \tag{64}$$

with

$$\boldsymbol{C}^{-1} = \begin{pmatrix} 35059 & -24031 \\ -24031 & 108300 \end{pmatrix} \tag{65}$$
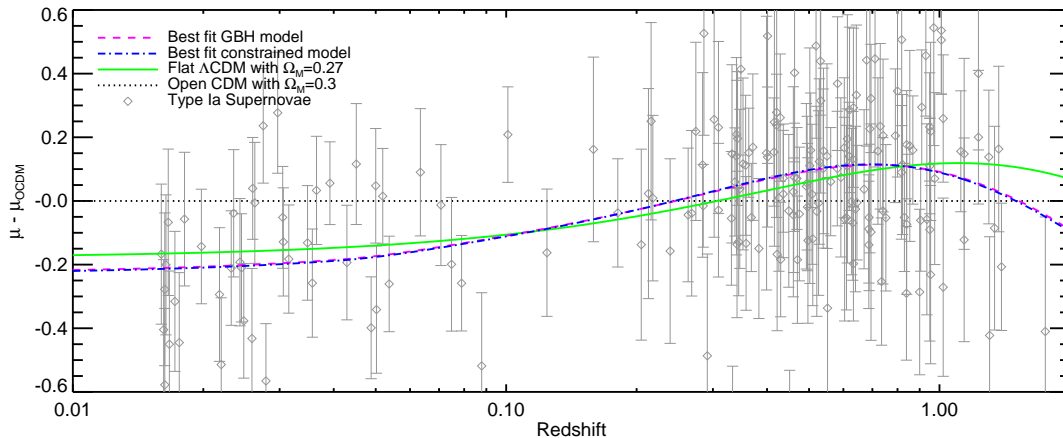
**Figure 4.** Apparent magnitude residuals for the two best fit LTB models, standard open CDM, and the best fit ΛCDM FRW models compared to Type Ia Supernovae data.

### 3.3. Type Ia Supernovae

We use the Type Ia Supernovae compilation by Davis et al. [32], which is a compilation of 192 SNIa consisting of 45 SNe from a nearby SNIa sample [33], 57 SNLS [34] and 60 ESSENCE [35] intermediate redshift SNe and 30 high redshift "Gold" SNe [36], with internally consistent magnitude offsets. The supernovae span the redshift range $z = 0.01 - 1.7$, and we use the magnitude residuals $\mu$ to constrain the LTB models. The residual $\mu$, and apparent and absolute magnitudes $m$ and $M$ are related to the luminosity distance $d_L$ as

$$\mu = m - M = 5 \log_{10} \left[ \frac{d_L}{1 Mpc} \right] + 25 \tag{66}$$

The exact absolute magnitude of a SNIa is unknown, and we include an arbitrary offset $\mu_0$, when calculating $\chi^2$ for the model fit to the observed SNIa

$$\chi^2_{\text{SNIa}} = \sum_i \frac{\left[ \mu_i^{\text{obs}} - (\mu^{\text{model}}(z_i) + \mu_0) \right]^2}{\sigma_i^2} \tag{67}$$

where $\mu_0$ is determined by minimising $\chi^2_{\text{SNIa}}$. $\mu$ has a logarithmic dependence on $d_L$, and the zero point $\mu_0$ is degenerate with the local overall scale of the expansion rate ($H_{\text{in}}$ in the GBH model, and $H_0$ in the constrained model, see Figs. 8 and 6).

Even though the Supernova data set is by far the largest of the three, the error bars on individual SNe are large, and internally there is a large scatter, as can be appreciated in Fig. 4, where the residuals are compared to the best fit GBH LTB models, and the open CDM and ΛCDM FRW models. Note that the predicted curves for the best fit GBH model and the best fit ΛCDM model start to deviate significantly beyond redshift $z = 1$, and therefore it would be extremely useful to have a complete Supernovae data set at high redshifts, which could help discard one of the models against the other one.

The three data sets discussed above are obtained through different means, and relate to different physical observations, and hence they are not correlated in any way. This independence allow us to find the total likelihood by simply multiplying the individual likelihood functions.

### 3.4. Priors

Even though we do not include them in the likelihood analysis, we still require our models to obey three additional priors: Two of them concern the local universe, and as such are priors at $z = 0$. They are the observed lower age limit on globular clusters in the Milky Way of 11.2 Gyr [37] (2-$\sigma$ limit) and the HST key project [38] measure of the *local* value for the Hubble parameter $H_{\rm in} = 72 \pm 8$ (1-$\sigma$ limit). The third prior is the gas fraction as observed in clusters of galaxies. This is a very powerful observation for limiting alternative models: Clusters of galaxies sit at the bottom of deep gravitational potential wells, and supposedly the gas fraction is representative for the universe as a whole, because neither gas nor dark matter can escape out of the potential well. This universal prior can be compared to the gas fraction we deduce far away from the void, by combining the WMAP satellite and Big Bang Nucleosynthesis bound on the physical baryon density $\omega_b = \Omega_b H_{\rm eff}^2 = 0.0223$ with the physical matter density at infinity $\omega_m = \Omega_{\rm out} H_{\rm eff}^2 = H_{\rm eff}^2$. The current observational limits are $f_{\rm gas} = \omega_b/\omega_m = 0.1104 \pm 0.0016 \pm 0.1$ (random+systematic) [39], while for our best fit models (see Table 2) we find $f_{\rm gas} = 0.127 - 0.134$ in agreement at 2-$\sigma$ with observations.

| Model | $H_0$ | $H_{\rm in}$ | $H_{\rm out}$ | $\Omega_{\rm in}$ | $r_0$ | $\Delta r$ |
|---|---|---|---|---|---|---|
| units | 100 km s$^{-1}$ Mpc$^{-1}$ | | | | Gpc | $r_0$ |
| GBH | $-$ | $0.5 - 0.85$ | $0.30 - 0.70$ | $0.05 - 0.35$ | $0.3 - 4.5$ | $0.1 - 0.9$ |
| Constrained | $0.50 - 0.95$ | $0.4 - 0.89$ | $0.33 - 0.63$ | $0.05 - 0.35$ | $0.5 - 4.5$ | $0.1 - 0.9$ |

**Table 1.** Priors used when scanning the parameters of the two models. In the constrained model $H_0$ is only a pre factor for $H_0(r)$ and the span of $H_{\rm in}$ and $H_{\rm out}$ are derived from the priors on $\Omega_{\rm in}$ and $H_0$.

## 4. Analysis and results

To test the full and the constrained GBH LTB model, we have performed a parameter scan over the models and for each set calculated the $\chi^2$. The priors are given in table 1, and have been chosen to encompass the best fit 2-$\sigma$ limits, except where large degeneracies exist, and also to be reasonable, taking into account the HST key project [38], and acceptable matter densities.
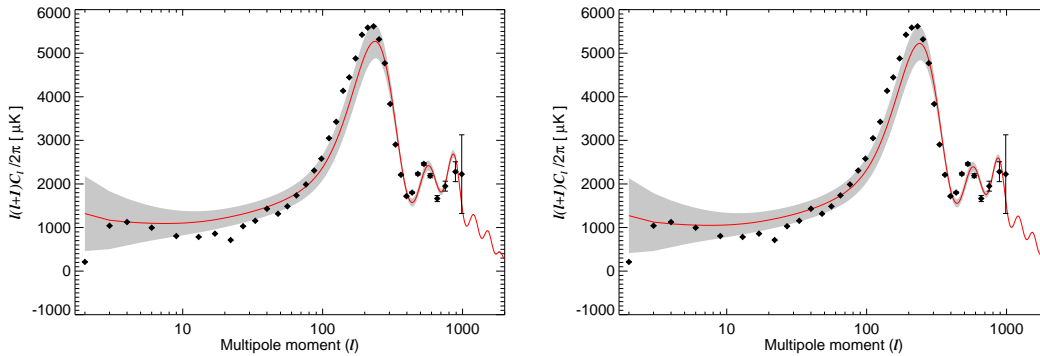
**Figure 5.** To the left/right the CMB spectrum for the best fit GBH/constrained-GBH model (red line) compared to WMAP3 data (diamonds) [41], and including cosmic variance (grey shading).

### 4.1. The best fit models

In table 2 are given the best fit for the two models. It is interesting to notice that both have very similar values, and in fact this seems to hint that current data prefer the simpler constrained model with a homogeneous big bang. Both best fit models have local Hubble rates on the low side but still in agreement with the HST project, and the local time to Big Bang is well inside the limits given by globular clusters.

The best fit models both give an excellent luminosity redshift distance relation, that are in as good an accordance with current Type Ia SNe as the $\Lambda$CDM model (see Fig. 4). This comes as no surprise: LTB models can be constructed that fit *any* luminosity-redshift relation [40]. Our model fit is done though under the simultaneous constraints of the other probes, and as such is more constrained. In the transition zone between the void and the surrounding Einstein-de Sitter space (at $r \sim r_0$) there is a significant (up to $\sim$10%) difference between $H_T(r)$, which is related to $d_L$, important for supernova observations, and $H_L(r)$, important for the longitudinal part of the Baryon Acoustic Oscillations (see Fig. 1). This difference marks a fundamental observational signature between LTB and FRW models. A set of very well observed Type Ia SNe at $z$ $0.1 - 0.2$, such as the SDSS II SN survey [23], together with the BAO observations already done at similar redshifts, will put strain on either model.

Because we currently do not have a full perturbation theory for LTB space times, we were not able to make a full likelihood analysis comparing our model to all the WMAP data. Nonetheless, to get an idea of how bad the models fit the full body of WMAP temperature anisotropy observations, we have calculated a standard temperature anisotropy spectrum using as input $H_{\text{eff}}$ and $\Omega = \Omega_{\text{out}} = 1$ (see Fig. 5). Even though we fix the physical baryon density, and only fit the first peak of the CMB, the obtained model is not too bad, and it is reassuring that other people have proposed Einstein-de Sitter models that do fit the WMAP3 CMB observations using a non standard primordial spectrum and a hot neutrino component (e.g. [42]). Very

recently an LTB model similar to ours was proposed [43] and the authors managed to make a reasonable fit to the full WMAP TT and TE data by adding a running of the tilt in the primordial spectrum. In a more complete analysis at low $l$-values and large angles one could expect an effect similar to that of a cosmological constant, since we have a non-trivial curvature at low redshifts, and hence an even better fit that do not have to rely on ad hoc features or a large running of the tilt in the primordial power spectrum may indeed be possible.

## 4.2. Likelihood contours and degeneracies

We have marginalised over different dimensions in parameter space by integrating over the likelihood, given as $\mathcal{L} \propto \exp(-\chi^2/2)$. The marginalised 1-$\sigma$ and 2-$\sigma$ likelihoods for the individual data sets, and also the 3-$\sigma$ limits for the combined data sets are shown in Figs. 8 and 6.

In the normal $\Lambda$CDM model, if $\omega_b$ is fixed, there is a well known strong degeneracy between $\Omega_m$ and $H_0$[44] for a given size of the sound horizon on the sky $\theta_A$. In our model the relevant $\Omega_m$ for the CMB is $\Omega_{out} = 1$, that fixes the size of the sound horizon, and we have also fixed $\omega_b$. Then the size of $\theta_A$ depends essentially on $H_0$ or $H_{in}$, which is reflected in the likelihood constraint from CMB on Hubble rates as seen in the figures. Nonetheless we can to some extent change $d_A$ by introducing curvature, allowing us to choose a higher value for $H_{in}$ or $H_0$, either by having a large void size, $r_0$, or making the void very underdense $\Omega_{in} \ll 1$. This can be seen by the widening of the 2-$\sigma$ limit in the $H$-$r_0$ plot for large values of $r_0$, and the asymmetric 2-$\sigma$ errors in the $H$-$\Omega_{in}$ plots.

$\Omega_{in}$ and $r_0$ are the major parameters determining the luminosity-redshift relation, and are hence constrained by the Type Ia SNe and the BAO. While only the relative value of Hubble rate play a role for the SNe, the BAO does limit $H$, and there is some strain between the BAO and the Type Ia SNe, as seen in the $\Omega_{in}$-$r_0$ plots.

An obvious degeneracy is that of $r_0$ and $\Delta r/r_0$ because the effect of a larger void can also be obtained by making a smoother, and hence broader, transition. Current data does not have any sensitivity to $H_{out}$, because it mainly affects the Hubble rate at very high redshift, where no good observational data exist. The relative transition width $\Delta r/r_0$ is also not very well constrained. The only thing we can deduce, in agreement with the good fit to the data given by the $\Lambda$CDM model, is that no sudden transition is allowed. The lower limit on $\Delta r/r_0$ is mainly limited by the Type Ia SN data, and to a lesser extent the BAO.

It should be stressed though, that even though our LTB models give very good fits with $\chi^2$ that are comparable to that of the $\Lambda$CDM model, current data *do* put significant constraints on the models, and they will probably be challenged by new observational data in the near future, and can be falsified.

| Model | $H_0$ | $H_{in}$ | $H_{out}$ | $H_{eff}$ | $\Omega_{in}$ | $r_0$ | $\Delta r$ | $t_{BB}$ |
|---|---|---|---|---|---|---|---|---|
| units | | 100 km s$^{-1}$ Mpc$^{-1}$ | | | | Gpc | $r_0$ | Gyr |
| GBH | − | 0.58±0.03 | 0.49±0.2 | 0.43 | 0.13±0.06 | 2.3±0.9 | 0.62(>0.20) | 14.8 |
| Constrained | 0.64±0.03 | 0.56 | 0.43 | 0.42 | 0.13±0.06 | 2.5±0.7 | 0.64(>0.21) | 15.3 |

**Table 2.** Best fit values with 2-$\sigma$ error bars for the two models. The likelihood contours are not closed for $\Delta r$, and only a lower limit can be given. In the GBH model $H_{out}$ is unconstrained. For the central values of the other four parameters $H_{out} = 0.49$ minimises $\chi^2$. Notice that naturally the best fit GBH model and the constrained model give similar best fit values, and error bars. Ie. among all the different GBH models a model with a homogeneous Big Bang is preferred.
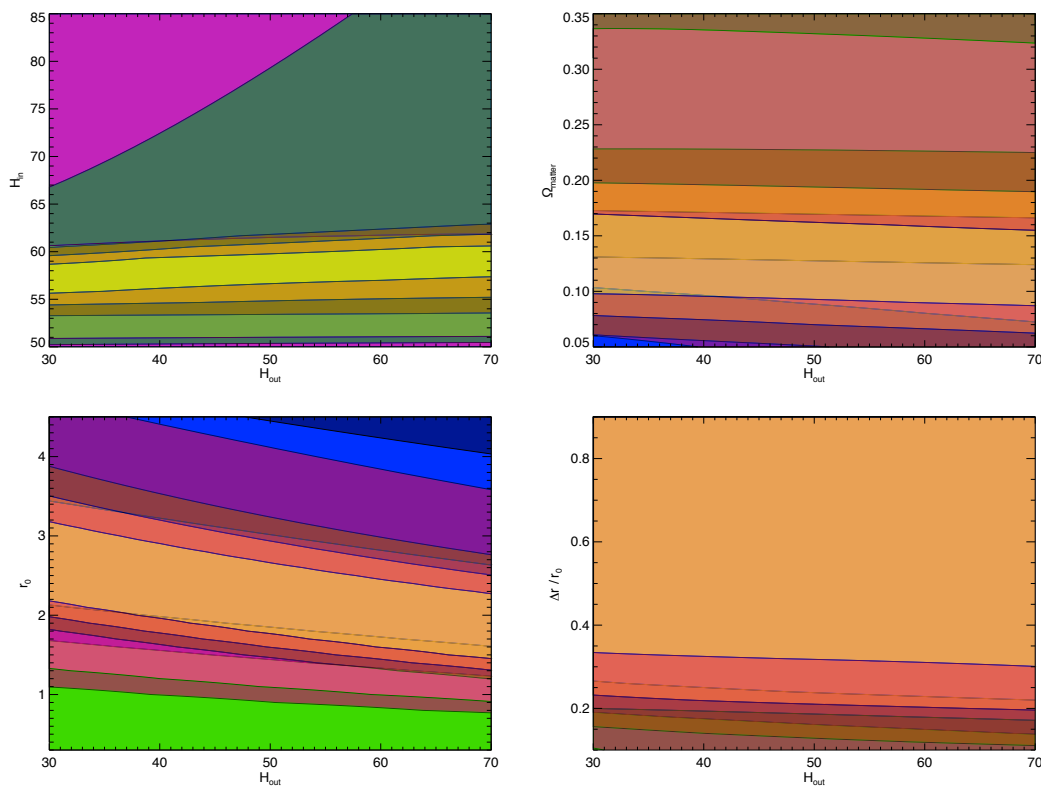


**Figure 6.** Likelihoods for the GBH model: The likelihood for the combined data set is shown in yellow with 1-, 2-, and 3-$\sigma$ contours, while the individual SNIa, BAO, and CMB data sets are shown in blue, purple, and green respectively with 1- and 2-$\sigma$ contours.

*4.3. Bayesian analysis*

In this section we would like to find out whether a homogeneous FRW model of the universe (including the accelerated expansion in terms of a vacuum energy with constant equation of state $w$) can be used with confidence when analysing present cosmological data, or should we rather be more general and assume an inhomogeneous LTB model of the universe?
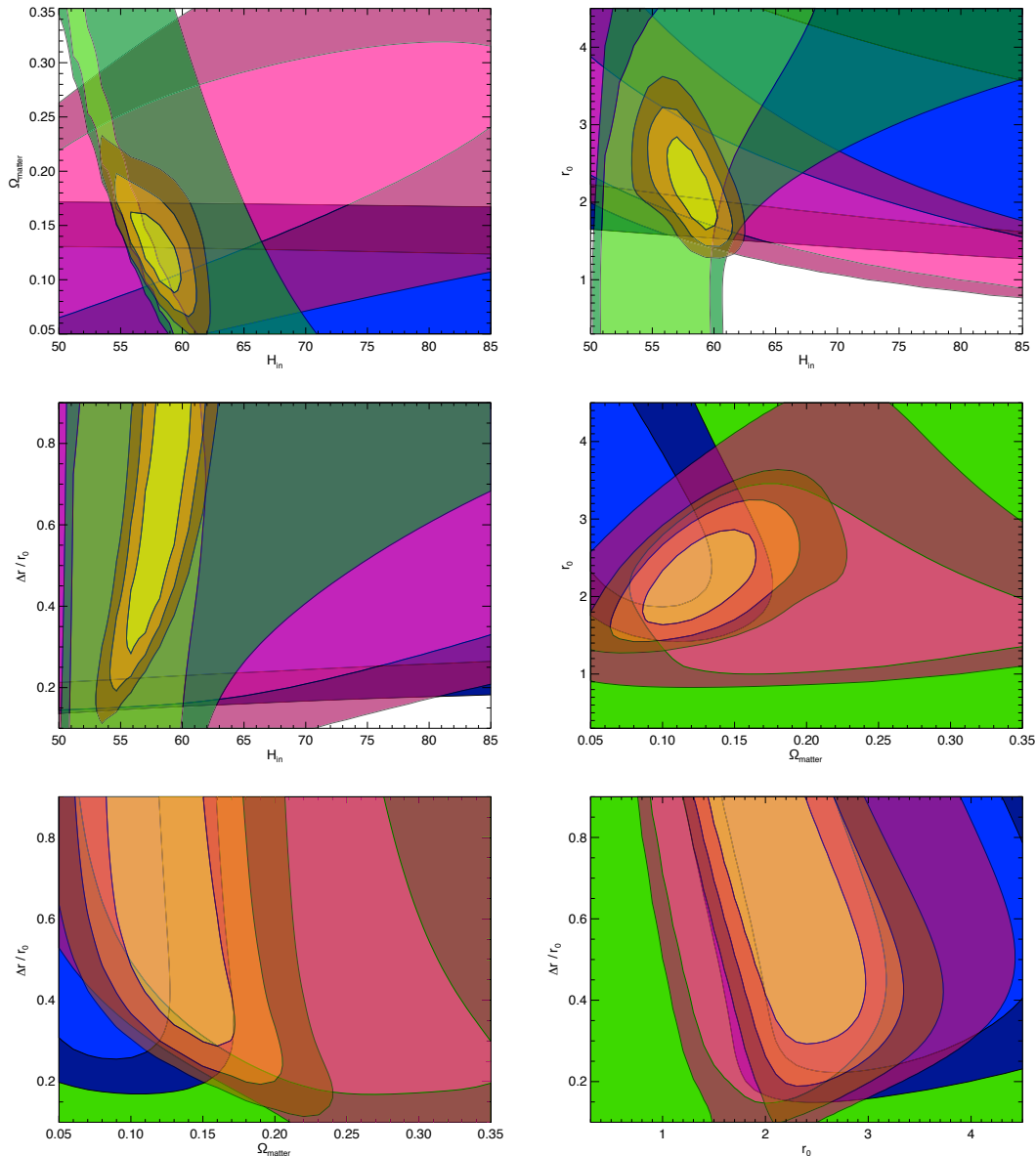
**Figure 7.** . . . Figure 6 continued.

The standard frequentist analysis of parameter estimation, given a set of data, is not very useful for model selection, since it is difficult to compare models with different number of parameters. For a discussion about probability theory and model selection see Refs. [45, 46, 47, 48]. For instance, the usual method of comparing minimum $\chi^2$ per effective degree of freedom normally misses the point and is not very decisive. Other methods to decide which model gives the best description, given the data, include various Information Criteria, e.g. Akaike [49] and Bayesian [50], which use more or less *ad hoc* formulae without much justification and normally do not compare well among eachother. However, in the last few years there has been a flourishing of several independent analysis based on the Bayesian evidence associated with a given likelihood and a given
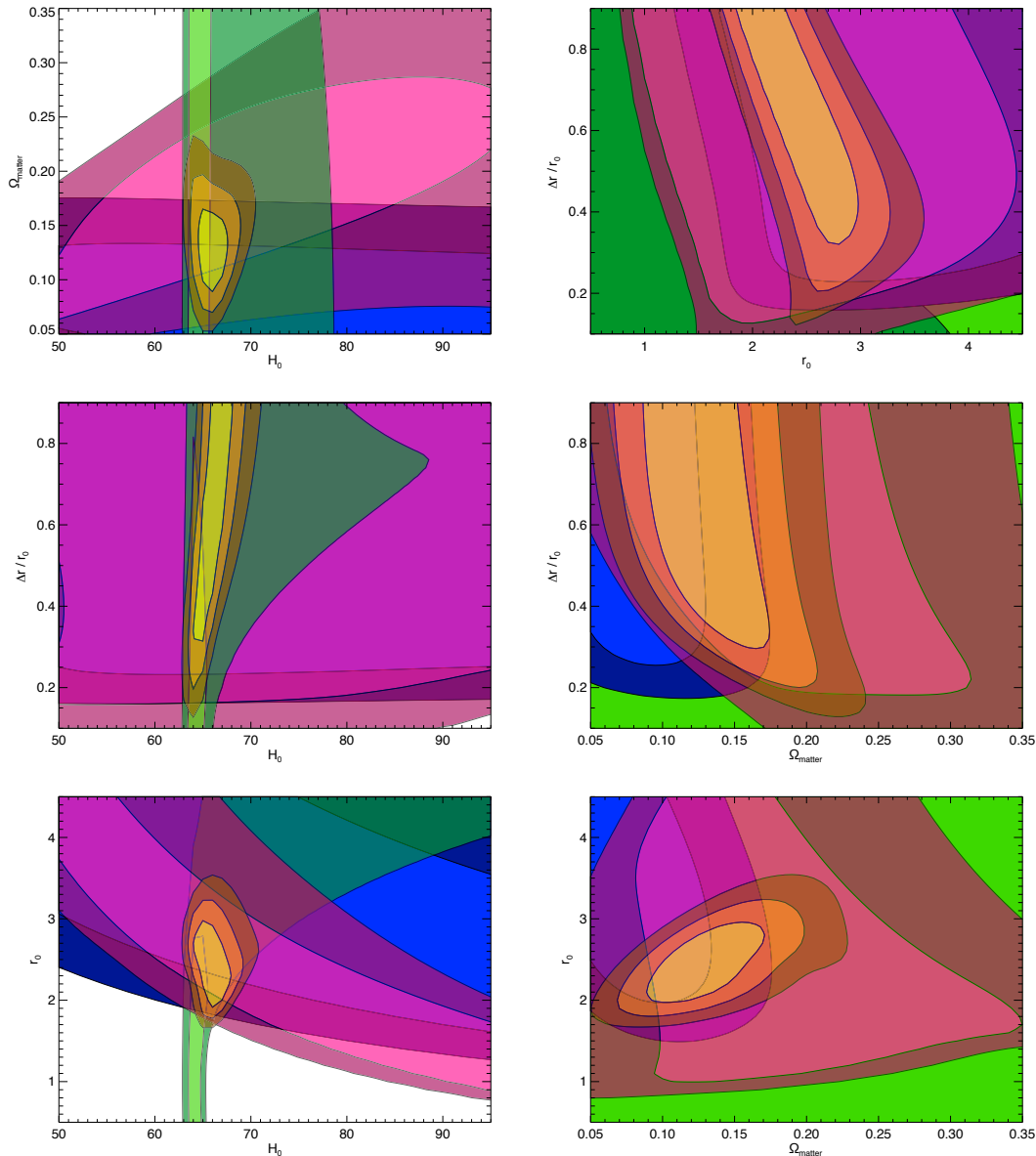
**Figure 8.** Likelihoods for the constrained model: The likelihood for the combined data set is shown in yellow with 1-, 2-, and 3-σ contours, while the individual SNIa, BAO, and CMB data sets are shown in blue, purple, and green respectively with 1- and 2-σ contours.

cosmological model, within some given priors, both theoretical and observational, see e.g. Refs. [51, 52, 53, 54].

The Bayesian evidence is based on Bayes theorem, which relates the posterior distribution $\mathcal{P}(\theta, \mathcal{M}|\mathbf{D})$ for the parameters $\theta$ of the model $\mathcal{M}$ given the data $\mathbf{D}$, in terms of the likelihood distribution function $\mathcal{L}(\mathbf{D}|\theta, \mathcal{M})$ within a given set of priors $\pi(\theta, \mathcal{M})$,

$$\mathcal{P}(\theta, \mathcal{M}|\mathbf{D}) = \frac{\mathcal{L}(\mathbf{D}|\theta, \mathcal{M})\, \pi(\theta, \mathcal{M})}{E(\mathbf{D}|\mathcal{M})}, \tag{68}$$

where $E$ is the Bayesian evidence, that is the average likelihood over the priors,

$$E(\mathbf{D}|\mathcal{M}) = \int d\theta \; \mathcal{L}(\mathbf{D}|\theta, \mathcal{M}) \, \pi(\theta, \mathcal{M}) \,. \tag{69}$$

The prior distribution functions contain all the information about the parameters *before* observing the data, e.g. our theoretical prejudices, our physical intuition about the model, the ranges of parameters obtained from previous experiments, etc. The Bayesian evidence is very useful because it allows a comparison of models within a complete set $\mathcal{M}_{i=1...N}$ (in our case, N=2). We can compute the posterior probability for each hypothesis (model) given the data $\mathbf{D}$ using again Bayes theorem, $\mathcal{P}(\mathcal{M}_i|\mathbf{D}) \propto E(\mathbf{D}|\mathcal{M}_i)\,\pi(\mathcal{M}_i)$, where $E(\mathbf{D}|\mathcal{M}_i)$ is the evidence of the data under model $\mathcal{M}_i$ and $\pi(\mathcal{M}_i)$ is the prior probability of the $i$-th model *before* we see the data, usually taken to be identical, i.e. $\pi(\mathcal{M}_{i=1...N}) = 1/N$. Finally, the ratio of the evidences for two competing models is called the *Bayes factor*,

$$B_{ij} \equiv \frac{E(\mathbf{D}|\mathcal{M}_i)}{E(\mathbf{D}|\mathcal{M}_j)} \,. \tag{70}$$

This expression provides a mathematical representation of Occam's razor, because more complex models tend to be less predictive, lowering their average likelihood (within the priors) in comparison with simpler, more predictive models. Complex models can only be favoured if they are able to provide a significantly improved fit to the data. In simple cases where different models give vastly different maximum likelihoods there is no need to employ model selection techniques because they provide only minor corrections to the standard inference, but they are essential when the difference between maximum likelihoods is only marginal, as will be the case at hand. The Bayes factor (70) is then used to give evidence of (i.e. favour) the model $\mathcal{M}_i$ against the model $\mathcal{M}_j$ using the so called Jeffreys' scale, a particular interpretation of the Bayes factor which strengthens its veridic roughly each time the logarithm $\ln B_{ij}$ increases by one unit, from 0 (undecisive) to greater than 5 (strongly ruled out).

Unfortunately, the computation of the Bayesian evidence (69) is rather involved and typically requires extensive computational power, unless the number of parameters is significantly reduced. When the likelihood of the data given the model parameters is a single isolated peak, far from the edges of the prior ranges, then there is a simple approximation to the logarithm of the Bayesian evidence,

$$\ln E = \ln \mathcal{L}_{\max} - \ln A - \sum_i^n \ln \Delta\theta_i \,, \tag{71}$$

where $A$ is the normalisation of the likelihood, and $\Delta\theta_i = b_i - a_i$ is the range of parameter $\theta_i \in [a_i, b_i]$, $i = 1 \ldots n$. Moreover, for the case of a Gaussian likelihood,

$$\mathcal{L}(\theta) = A \, \exp\left[ -\frac{1}{2}\mathbf{x}^{\mathrm{T}} C^{-1}\mathbf{x} \right] ,$$

we find $A = (2\pi)^{-n/2}/\sqrt{\det C}$, where $C$ is the covariance matrix and $x_i = \theta_i - \bar{\theta}_i$. It is clear that whenever the prior ranges are too big for the likelihood, the Bayesian evidence

is penalised. Moreover, the more parameters there are, the larger the difference in $\ln E$, and the larger the logarithm of the Bayes factor, as expected.

We will now apply this discussion to the case at hand. We will compare the standard flat $\Lambda$CDM model with a constant equation of state parameter, $w$, while fixing all other cosmological parameters but $\Omega_M$. Thus our FRW model has here 2 parameters, which we believe are the most constraining, since others like the local rate of expansion do not provide significant extra information. We performed a calculation of the minimum $\chi^2$ within a grid of 5000 models, where $w \in [-2.0, 0.0]$ and $\Omega_M \in [0.0, 0.6]$. The maximum likelihood corresponds to a $\chi^2_{\min}(\Lambda CDM) = 197.05$ for $w = -1.005$ and $\Omega_M = 0.276$.

On the other hand, the constrained GBH model has 4 independent parameters, the local rate of expansion $H_0 = 100\,h$ km/s/Mpc, the local matter fraction $\Omega_m \equiv \Omega_M(0)$, the transition distance $r_0$, and the width $\Delta r/r_0$, providing a grid of several million models within the ranges $h \in [0.50, 0.95]$, $\Omega_m \in [0.05, 0.35]$, $r_0 \in [0.5, 4.5]$ and $\Delta r/r_0 \in [0.1, 0.9]$. We found that the maximum likelihood corresponds to a $\chi^2_{\min}(GBH) = 197.845$ for $h = 0.659$, $\Omega_m = 0.124$, $r_0 = 2.47$ Gpc and $\Delta r/r_0 = 0.638$.

At face value it seems that the inhomogeneous model provides as good a fit to the data as the FRW one. If we compute the usual minimum $\chi^2$ per effective number of degrees of freedom (i.e. the number of data points minus the number of parameters), we find

$$\chi^2_{\min}(\Lambda CDM)/d.o.f. = 1.021\,, \qquad \chi^2_{\min}(GBH)/d.o.f. = 1.036\,, \qquad (72)$$

so that both models seem excellent descriptions of the data, the first one being slightly better. However, there are other indicators more appropriate for model comparison, like the (corrected) Akaike Information Criterion ($AIC$), computed as

$$AIC = \chi^2_{\min} + 2k + \frac{2k(k-1)}{N - k - 1}\,, \qquad (73)$$

where $k$ is the number of parameters and $N$ is the number of data points. In our case this gives $AIC(\Lambda CDM) = 201.1$, while $AIC(GBH) = 206.0$, which would clearly favour the homogeneous FRW model. On the other hand, if we choose to compare models with the Bayesian Information Criterion ($BIC$), computed as

$$BIC = \chi^2_{\min} + k \ln N\,, \qquad (74)$$

we find $BIC(\Lambda CDM) = 207.6$, while $BIC(GBH) = 218.9$, which would very strongly favour the homogeneous FRW model. Clearly, neither method gives a good assessment for choosing among models. This is the reason why the Bayesian evidence has been used recently in the context of model comparison.

If we compute the Bayes factor (70) by performing the integral of the likelihood over the priors, (69), we find

$$\ln E(\Lambda CDM) = -103.1\,, \qquad \ln E(GBH) = -106.7\,, \qquad (75)$$

and therefore the logarithm of the Bayes factor is $\ln B_{12} = 3.6$, which clearly favours the homogeneous FRW model against the GBH-LTB model. It seems that the bayesian evidence method discards significantly, but not very strongly, the inhomogeneous model

versus the usual FRW model. It is possible that, in the future, better data sets and stronger priors on cosmological parameters may discard once and for all the inhomogeneous model. For the moment, a local void with a size of several Gpc, with matter well below average, and a local rate of expansion of 71 km/s/Mpc, can account for both the distant (CMB), intermediate (SNIa) and local (BAO) data sets.

## 5. Discussion and Conclusions

We have shown that present observations do not exclude the possibility that we live close to the center of a large void. This is a appealing possibility which effectively gets rid of the necessity to introduce an ad hoc cosmological constant in our model of the universe. Moreover, it is consistent with early universe cosmology in terms of inflationary initial conditions for the origin of large scale structures. Perhaps these voids arise due to large non-perturbative inhomogeneities associated with the stochastic nature of the inflaton evolution [15], or due to large non-gaussianities in the primordial spectrum coming from inflation that could arise due to phase transitions or in multifield inflation [55, 56]. In fact, we already know there can be other voids in our local patch of the universe, with a Gpc scale, as exemplified by the observed cold spot in the CMB [14].

We have analysed the likelihood of such an interpretation of the present acceleration of the universe, using data from the Cosmic Microwave Background (on large scales), Supernova Ia (at intermediate scales), Baryon Acoustic Oscillations, the present age and the local rate of expansion (at small scales). All the data seems to be consistent at the 95% confidence level with a local void of size around 2.5 Gpc, within an Einstein-de Sitter universe on large scales, without the need to introduce a cosmological constant. The apparent acceleration of the universe can be interpreted here as due to the curved path of photons in this locally open universe.

We have performed a Bayesian analysis in order to compare two competing models, the predominant $\Lambda$CDM model and our GBH inhomogeneous model. While the usual frequentists analysis does not discard the GBH model against the $\Lambda$CDM model, there seems to be strong but not decisive (bayesian) evidence against the GBH model. It is possible that in the near future, with much better cosmological data on large scale structures and an extended set of supernovae at intermediate and high redshift, we may be able to constrain and definitely rule out the inhomogeneous LTB model. We should also mention that the data seems to favour a homogeneous Big Bang since the constrained GBH model gives the same likelihood contours and minimum $\chi^2$ than the unconstrained model, while having one parameter less.

At the moment we are studying the effect that a generic LTB model has on the growth of structure in order to constrain further the GBH model with data from ISW-LSS correlations and the Lyman-$\alpha$ forest within the Alcock-Paczynski-test analysis [31].

In conclusion, we cannot discard that we live in an inhomogeneous local void within an asymptotically Einstein-de Sitter universe. The possibility that we have misinterpreted the present acceleration and that the cosmological constant is nothing

but a mirage has been addressed recently [57, 58, 59]. We have added to the discussion the comparison with a large, albeit incomplete, set of cosmological observations, and the bayesian analysis appropriate for model selection. We hope in the future to provide further constraints on the model and possibly rule it out.

## Acknowledgements

## References

[1] `http://www.darkenergysurvey.org`.
[2] `http://www.aip.org/web_bin/pt/vol-58/iss-8/p53.shtml`.
[3] George Lemaître. "The Expanding Universe". *Gen. Rel. Grav.*, 29:641–680, 1997.
[4] Richard C. Tolman. "Effect of imhomogeneity on cosmological models". *Proc. Nat. Acad. Sci.*, 20:169–176, 1934.
[5] H. Bondi. "Spherically symmetrical models in general relativity". *Mon. Not. Roy. Astron. Soc.*, 107:410–425, 1947.
[6] Idit Zehavi, Adam G. Riess, Robert P. Kirshner, and Avishai Dekel. "A Local Hubble Bubble from SNe Ia?". *Astrophys. J.*, 503:483, 1998, astro-ph/9802252.
[7] Kenji Tomita. "Anisotropy of the Hubble Constant in a Cosmological Model with a Local Void on Scales of 200 Mpc". 2000, astro-ph/0005031.
[8] Kenji Tomita. "A Local Void and the Accelerating Universe". *Mon. Not. Roy. Astron. Soc.*, 326:287, 2001, astro-ph/0011484.
[9] Kenji Tomita. "Analyses of Type Ia Supernova Data in Cosmological Models with a Local Void". *Prog. Theor. Phys.*, 106:929–939, 2001, astro-ph/0104141.
[10] William J. Frith, G. S. Busswell, R. Fong, N. Metcalfe, and T. Shanks. "The Local Hole in the Galaxy Distribution: Evidence from 2MASS". *Mon. Not. Roy. Astron. Soc.*, 345:1049, 2003, astro-ph/0302331.
[11] G. S. Busswell et al. "The Local Hole in the Galaxy Distribution: New Optical Evidence". *Mon. Not. Roy. Astron. Soc.*, 354:991, 2004, astro-ph/0302330.
[12] Patricio Vielva, E. Martinez-Gonzalez, R. B. Barreiro, J. L. Sanz, and L. Cayon. "Detection of non-Gaussianity in the WMAP 1-year data using spherical wavelets". *Astrophys. J.*, 609:22–34, 2004, astro-ph/0310273.
[13] M. Cruz, M. Tucci, E. Martinez-Gonzalez, and P. Vielva. "The non-Gaussian Cold Spot in WMAP: significance, morphology and foreground contribution". *Mon. Not. Roy. Astron. Soc.*, 369:57–67, 2006, astro-ph/0601427.
[14] Marcos Cruz, L. Cayon, E. Martinez-Gonzalez, P. Vielva, and J. Jin. "The non-Gaussian Cold Spot in the 3-year WMAP data". *Astrophys. J.*, 655:11–20, 2007, astro-ph/0603859.
[15] Andrei D. Linde, Dmitri A. Linde, and Arthur Mezhlumian. "Do we live in the center of the world?". *Phys. Lett.*, B345:203–210, 1995, hep-th/9411111.

[16] Andrei D. Linde, Dmitri A. Linde, and Arthur Mezhlumian. "From the Big Bang theory to the theory of a stationary universe". *Phys. Rev.*, D49:1783–1826, 1994, gr-qc/9306035.

[17] Juan Garcia-Bellido, Andrei D. Linde, and Dmitri A. Linde. "Fluctuations of the gravitational constant in the inflationary Brans-Dicke cosmology". *Phys. Rev.*, D50:730–750, 1994, astro-ph/9312039.

[18] Kari Enqvist and Teppo Mattsson. "The effect of inhomogeneous expansion on the supernova observations". *JCAP*, 0702:019, 2007, astro-ph/0609120.

[19] Kari Enqvist. "Lemaitre-Tolman-Bondi model and accelerating expansion". 2007, arXiv:0709.2044 [astro-ph].

[20] Havard Alnes, Morad Amarzguioui, and Oyvind Gron. "An inhomogeneous alternative to dark energy?". *Phys. Rev.*, D73:083519, 2006, astro-ph/0512006.

[21] Eric V. Linder and Adrian Jenkins. "Cosmic Structure and Dark Energy". *Mon. Not. Roy. Astron. Soc.*, 346:573, 2003, astro-ph/0305286.

[22] Eric V. Linder. "Cosmic growth history and expansion history". *Phys. Rev.*, D72:043529, 2005, astro-ph/0507263.

[23] `http://sdssdp47.fnal.gov/sdsssn/sdsssn.html`.

[24] `http://www.ice.csic.es/pau`.

[25] D. N. Spergel et al. "Wilkinson Microwave Anisotropy Probe (WMAP) three year results: Implications for cosmology". *Astrophys. J. Suppl.*, 170:377, 2007, astro-ph/0603449.

[26] Daniel J. Eisenstein and Wayne Hu. "Baryonic Features in the Matter Transfer Function". *Astrophys. J.*, 496:605, 1998, astro-ph/9709112.

[27] Daniel J. Eisenstein et al. "Detection of the Baryon Acoustic Peak in the Large-Scale Correlation Function of SDSS Luminous Red Galaxies". *Astrophys. J.*, 633:560–574, 2005, astro-ph/0501171.

[28] Teppei Okumura et al. "Large-Scale Anisotropic Correlation Function of SDSS Luminous Red Galaxies". 2007, arXiv:0711.3640 [astro-ph].

[29] Will J. Percival et al. "Measuring the Baryon Acoustic Oscillation scale using the SDSS and 2dFGRS". 2007, arXiv:0705.3323 [astro-ph].

[30] Nikhil Padmanabhan et al. "The Clustering of Luminous Red Galaxies in the Sloan Digital Sky Survey Imaging Data". *Mon. Not. Roy. Astron. Soc.*, 378:852–872, 2007, astro-ph/0605302.

[31] Alicia Bueno, Juan García-Bellido, and Troels Haugboelle. "Linear perturbation theory in LTB models". in preparation.

[32] Tamara M. Davis et al. "Scrutinizing exotic cosmological models using ESSENCE supernova data combined with other cosmological probes". *Astrophys. J.*, 666:716, 2007, astro-ph/0701510.

[33] Saurabh Jha, Adam G. Riess, and Robert P. Kirshner. "Improved Distances to Type Ia Supernovae with Multicolor Light Curve Shapes: MLCS2k2". *Astrophys. J.*, 659:122–148, 2007, astro-ph/0612666.

[34] Pierre Astier et al. "The Supernova Legacy Survey: Measurement of Omega_M, Omega_Lambda and w from the First Year Data Set". *Astron. Astrophys.*, 447:31–48, 2006, astro-ph/0510447.

[35] W. Michael Wood-Vasey et al. "Observational Constraints on the Nature of the Dark Energy: First Cosmological Results from the ESSENCE Supernova Survey". *Astrophys. J.*, 666:694, 2007, astro-ph/0701041.

[36] Adam G. Riess et al. "New Hubble Space Telescope Discoveries of Type Ia Supernovae at $z > 1$: Narrowing Constraints on the Early Behavior of Dark Energy". *Astrophys. J.*, 659:98, 2006, astro-ph/0611572.

[37] Lawrence M. Krauss and Brian Chaboyer. "Age Estimates of Globular Clusters in the Milky Way: Constraints on Cosmology". *Science*, 299:65–70, 2003.

[38] W. L. Freedman et al. "Final Results from the Hubble Space Telescope Key Project to Measure the Hubble Constant". *Astrophys. J.*, 553:47–72, 2001, astro-ph/0012376.

[39] S. W. Allen et al. "Improved constraints on dark energy from Chandra X-ray observations of the largest relaxed galaxy clusters". 2007, arXiv:0706.0033 [astro-ph].

[40] Marie-Noelle Celerier. "Do we really see a cosmological constant in the supernovae data?". *Astron.*

*Astrophys.*, 353:63–71, 2000, astro-ph/9907206.

[41] G. Hinshaw et al. "Three-year Wilkinson Microwave Anisotropy Probe (WMAP) observations: Temperature analysis". *Astrophys. J. Suppl.*, 170:288, 2007, astro-ph/0603451.

[42] Paul Hunt and Subir Sarkar. "Multiple inflation and the WMAP 'glitches' II. Data analysis and cosmological parameter extraction". 2007, arXiv:0706.2443 [astro-ph].

[43] Stephon Alexander, Tirthabir Biswas, Alessio Notari, and Deepak Vaid. Local Void vs Dark Energy: Confrontation with WMAP and Type Ia Supernovae. 2007, arXiv:0712.0370 [astro-ph].

[44] L. Page et al. First Year Wilkinson Microwave Anisotropy Probe (WMAP) Observations: Interpretation of the TT and TE Angular Power Spectrum Peaks. *Astrophys. J. Suppl.*, 148:233, 2003, astro-ph/0302220.

[45] H. Jeffreys. "The theory of probability". Oxford U.P. (1998).

[46] E.T. Jaynes. "Probability Theory: the Logic of Science". Cambridge U.P. (2003).

[47] D.J.C. Mackay. "Information theory, inference and learning algorithms". Cambridge U.P. (2003).

[48] G. D'Agostini. "Bayesian reasoning in data analysis: A critical introduction". World Scientific (2003).

[49] Hirotugu Akaike. "A new look at the statistical model identification". *IEEE Transactions on Automatic Control*, 16 (6):716–723, 1974.

[50] G. Schwarz. "Estimating the dimension of a model". *Annals of Statistics*, 6 (2):461–464, 1978.

[51] Andrew R. Liddle. "How many cosmological parameters?". *Mon. Not. Roy. Astron. Soc.*, 351:L49–L53, 2004,

[52] Maria Beltran, Juan Garcia-Bellido, Julien Lesgourgues, Andrew R Liddle, and Anze Slosar. "Bayesian model selection and isocurvature perturbations". *Phys. Rev.*, D71:063532, 2005, astro-ph/0501477.

[53] David Parkinson, Pia Mukherjee, and Andrew R Liddle. "A Bayesian model selection analysis of WMAP3". *Phys. Rev.*, D73:123523, 2006, astro-ph/0605003.

[54] Roberto Trotta. "Applications of Bayesian model selection to cosmological parameters". *Mon. Not. Roy. Astron. Soc.*, 378:72–82, 2007, astro-ph/0504022.

[55] L. A. Kofman and Andrei D. Linde. Generation of Density Perturbations in the Inflationary Cosmology. *Nucl. Phys.*, B282:555, 1987.

[56] Xingang Chen, Richard Easther, and Eugene A. Lim. Generation and Characterization of Large Non-Gaussianities in Single Field Inflation. 2008, arXiv:0801.3295 [astro-ph].

[57] Teppo Mattsson. "Dark energy as a mirage". 2007, arXiv:0711.4264 [astro-ph].

[58] David L. Wiltshire. Dark energy without dark energy. 2007, arXiv:0712.3984 [astro-ph].

[59] Nan Li, Marina Seikel, and Dominik J. Schwarz. "Is dark energy an effect of averaging?". 2008, arXiv:0801.3420 [astro-ph].